Performance and stability improvements for dye-sensitized solar cells in the presence of luminescent coatings

Federico Bella [a, *], Gianmarco Griffini [b], Matteo Gerosa [a], Stefano Turri [b], Roberta Bongiovanni [a]

[a] Department of Applied Science and Technology — DISAT, Politecnico di Torino, Corso Duca degli Abruzzi 24, 10129 Torino, Italy
[b] Department of Chemistry, Materials and Chemical Engineering "Giulio Natta", Politecnico di Milano, Piazza Leonardo da Vinci 32, 20133 Milano, Italy

* Corresponding author.
E-mail address: federico.bella@polito.it (F. Bella).

1. Introduction

Dye-sensitized solar cells (DSSCs) have proven to be one of the most valuable third generation photovoltaic (PV) technology for the conversion of solar energy into electricity during the last twenty years [1]. The seminal work of O'Regan and Grätzel is the most cited article in the whole energy field [2], and more than 13,000 papers have been written to propose new materials, characterization techniques and large-scale implementation of DSSCs [3]. At pre-sent, efficiencies higher than 13% have been obtained on a labora-tory scale [4], but also the manufacture of flexible devices [5], the design of unconventional electrodes [6], and the fabrication of hybrid cells [7] are research topics of great interest.

However, a few important aspects still need to be addressed in order to make DSSCs even more attractive and reliable on the global energy market. First of all, investigations have been carried out mostly on organometallic dyes, but metal-free organic dyes are getting increasing attention in view of obtaining market-competitive devices [8]. Organic dyes do not contain any rare or noble metal, thus generating fewer concerns about resource limits, and have recently demonstrated to be able to produce a 12.5% ef-ficiency [9]. The second topic concerns the outdoor use of DSSCs, and therefore their resistance to meteorological phenomena, pollution and undesired UV radiation. Quite surprisingly, coatings have been developed almost exclusively for antireflective purposes, especially for silicon- and CdTe-based solar cells [10,11]. During the last two years, multifunctional coatings have also been designed for combined antireflective and self-cleaning purposes, and have been applied onto silicon and polymeric solar cells [12,13]. Even if polymers have been chosen as basic matter for coating preparation, also inorganic matrices (pure or mixed metal oxides) have been investigated [14]. However, despite the great academic and indus-trial efforts spent on DSSCs components, the development of functional coatings for improving the outdoor stability and per-formance of this type of third generation devices has been sur-prisingly neglected. Most of the research groups overlook this aspect, and only a small fraction of them apply a commercial antireflective coating on the fabricated PV cells [15]. Very recently, a couple of interesting works has been proposed on this matter. Park et al. prepared a superhydrophilic nanoparticle-based coating to be applied as anti-fogging layer [16], while Heo et al. fabricated a hydrophobic nanopatterned coating with antireflective and self-cleaning properties [17]. We think that the impact of these semi-nal works may trigger the interest of the scientific community on a very far ignored aspect of DSSC technology. In particular, the great potential of fluorinated polymer matrices has yet to be exploited in the DSSC field. Indeed, fluorinated polymers are a class of high-performance materials that rely on the superior strength (higher dissociation energy) of the carbon−fluorine bond compared to the carbon−hydrogen bond to achieve excellent durability, weather-ability, chemical and photochemical resistance [18−20]. The use of fluorinated polymer coatings for outdoor applications represents a consolidated way to achieve high weathering resistance and long-term durability in a variety of technological fields (e.g., architec-tural, nautical), and only very recently their application to the field of energy storage and conversion has also been demonstrated [21−23].

Our recent experimental research activities have been sepa-rately focused on the preparation of light-managing coatings for PV applications [23,24] and on the development of new materials for different PV technologies [25−27]. A very ambitious goal would be that of combining the ability of a coating to be easily-cleanable with a light-shifting (LS) effect promoted by the addition of an appro-priate luminophore to the coating system. Considering this latter point, a few recent articles reported on the use of rare earths as UV or visible light shifters [28−32]. However, such systems have two major flaws: 1) The luminophores (Y_2WO_6:Ln^{3+}, $NaYF_4$:Yb^{3+}/Er^{3+}, CaZnOS:Eu^{2+}, Y_2O_3:Er^{3+}) are composed of rare and expensive inorganic elements; 2) Aging studies on devices including these LS

systems are not presented, presumably because these inorganic materials are water soluble or suspendable, thus real outdoor ap-plications are not conceivable. A first example of a stable lumi-nescent system for DSSCs has been very recently proposed by our group, and consisted of a polymer coating containing a Europium complex as downshifter [33]. However, the presence of rare and expensive element such as Europium does not make this technol-ogy suitable for a large-scale trade.

In this work, we propose a multifunctional coating which can simultaneously be easy-cleaning and LS for application in organic DSSCs. In detail, the easy-cleaning ability is ascribed to the use of a fluoropolymeric matrix system that can be photocured in a few seconds, thus potentially enabling its use in large-scale production volumes. By the addition of a rare elements-free organic fluo-rophore, this coating is also able to serve as LS system by absorbing light in the UV portion of the solar spectrum and re-emitting it in the spectral region where the DSSC sensitizer shows a maximum absorption (Fig. 1). Since organic DSSC dyes often present a rela-tively narrow spectral breadth [34,35], our proof of concept shows the possibility to partly overcome this problem, by shifting otherwise-wasted and potentially harmful UV-photons to wave-lengths suitable for absorption by the DSSC device. The optimiza-tion of the LS-DSSC system allowed us to improve by 62% the efficiency of a DSSC prepared with the organic dye D131. Moreover, thanks to the UV-screening action of the rare elements-free fluo-rophore used in the LS-coating presented in this work, the often detected photo-oxidative degradation of the organic dye [36] could be prevented. Accordingly, an aging test conducted for more than 2000 h in real outdoor conditions revealed the excellent stability of the new LS-DSSC system presented in this work compared to control devices.

2. Experimental

2.1. Materials

The chloro-tri-fluoro-ethylene vinyl-ether (CTFE-VE) polymeric binder (Lumiflon LF-910LM) was obtained from Asahi Glass Com-pany Ltd., while 2-isocyanatoethyl methacrylate (IEM) was ob-tained from Showa Denko K.K. Both were used as received. The luminescent species employed in this work was Lumogen F Violet 570, purchased from BTC Europe.

As regards DSSC components, conducting glass plates (FTO glass, Fluorine doped Tin Oxide over-layer, sheet resistance 7 Ω sq^{-1}, purchased from Solaronix) were cut into 2 cm × 2 cm sheets and used as substrates for both the deposition of a TiO_2 porous film from a paste (DSL 18NR-AO, Dyesol) and the fabrication of platinized counter-electrodes. Sensitizing dye 2-[{4-[4-(2,2-diphenylethenyl)phenyl]-1,2,3,3a,4,8b-hexahydrocyclopento[b]indole-7-yl}methylidene]-cyanoacetic acid (D131) was purchased from Inabata Europe S.A.

All other reagents were purchased from Sigma Aldrich, unless otherwise stated.

2.2. Synthetic method

The CTFE-VE polymer was allowed to react with IEM to form the photocrosslinkable polyurethane precursor. In a typical synthesis, 40 g of CTFE-VE and 7.3 g of IEM were poured in stoichiometric ratio (OH/NCO = 1) into a three-necked round-bottomed flask equipped with a bubble condenser. Di-n-butyltin dilaurate (0.3 wt.%) was added successively to act as catalyst. The reaction was conducted in a nitrogen atmosphere and under vigorous magnetic stirring at 75 °C. The extent of reaction was controlled by monitoring the disappearance of the N=C=O stretching signal (2270 cm^{-1}) by
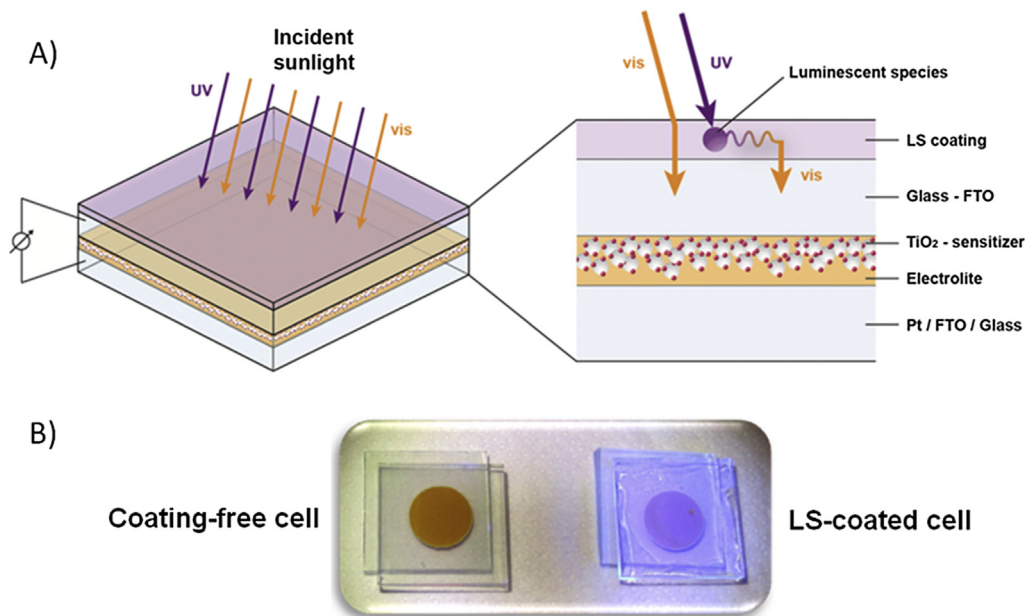
Fig. 1. A) Graphical representation of the working principle of the LS system presented in this work when applied on a DSSC device; B) Comparison between a coating-free and a V570-doped LS-DSSC when irradiated with UV light.

means of FTIR spectroscopy, and was found to be completed after about 6 h. The final product was diluted with chloroform ($CHCl_3$) to the desired concentration.

2.3. UV-curing process

In order to perform the UV-curing process, photopolymer precursor was exposed to UV-light (35 mW cm^{-2}, as measured by means of a UV Power Puck® II radiometer, EIT) coming from a medium pressure mercury lamp equipped with an optical guide (LC8, Hamamatsu) for 60 s. The UV irradiation was carried out under nitrogen flux, to prevent quenching of free-radicals by atmospheric oxygen. Darocur 1173 (Ciba Specialty Chemicals) was used as the photoinitiator (3 wt.%). UV-exposed polymer films were immersed in $CHCl_3$ for 5 min to preliminary evaluate the extent of UV-curing. The conversion of the UV-curing reaction was monitored by FTIR by depositing a film of polymer precursor onto a KBr disk via spin-coating and subsequently irradiating it with UV light for a given amount of time, followed by quenching in an ice bath to stop the curing reaction. The FTIR spectrum of the film was then collected. This procedure was repeated on the same polymer film for increasing UV-light exposure times, for a maximum of 120 s.

2.4. DSSC fabrication

Photoanodes preparation started with a cleaning process: FTO covered glasses were rinsed in acetone and ethanol in an ultrasonic bath for 10 min. Then, a TiO_2 paste layer with a circular shape was deposited on FTO by screen printing technique (AT-25PA, Atma Champ Ent. Corp.) and dried at 100 °C for 10 min on a hot plate. A sintering process at 525 °C for 30 min led to a nanoporous TiO_2 film with an average thickness of 8.5 μm, measured by profilometry (P.10 KLA-Tencor Profiler). The photoelectrodes were then soaked into a 0.5 mM D131 dye solution in a *tert*-butanol:acetonitrile 1:1 mixture for 5 h at ambient temperature, and finally washed with acetone to remove the unadsorbed dye. 0.5 mM of chenodeoxycholic acid (CDCA) as coadsorbent in the dye solution was added.

As regards the preparation of counter electrodes, 6 nm Pt thin films were deposited by sputtering (Q150T ES, Quorum Technologies Ltd) onto FTO glasses, previously cleaned with the same rinsing method described above.

For DSSC device fabrication, photoanode and counter electrode were assembled into a sealed sandwich type cell with a gap of a hot-melt ionomer film, Surlyn (60 μm, Du-Pont). The cell internal space was filled with electrolyte via vacuum backfilling. The liquid electrolyte consisted of 1-methyl-3-propylimidazolium iodide (MPII, 0.60 M), iodine (I_2, 50 mM), lithium iodide (LiI 0.10 M) and 4-*tert*-butylpyridine (TBP, 50 mM) in 3-methoxypropionitrile (MPN). The injection hole on the counter electrode was then sealed with a Surlyn sheet and a thin glass slice by heating.

The UV-curable photopolymer precursor was diluted to a concentration of 30 wt.% in $CHCl_3$. The amount of the luminescent species in the UV-curable fluoropolymer was varied between 0 wt.% and 10 wt.%. Each sealed DSSC was fixed onto a SPIN150 spin processor (SPS-Europe), and a few drops of the UV-curable precursor were placed on the external side of the photoanode. Samples were spin-coated at 1000 rpm for 45 s with an acceleration equal to 25 rpm s^{-1}, and subsequently UV-cured as reported above. The final thickness of the coating was 35 μm, which preliminary tests proved to be the best value for our purposes.

2.5. Characterization techniques

UV−vis and fluorescence spectroscopy were performed on UV-cured LM-coatings deposited onto glass/quartz substrates by spin-coating (WS-400B-NPP Spin-Processor, Laurell Technologies Corp.) at 1000 rpm for 40 s in air. UV−vis absorption spectra were recorded in air at room temperature in transmission mode by means of an Evolution 600 UV−vis spectrophotometer (Thermo Scientific). Fluorescence emission spectra were recorded in air at room temperature on a Jasco FP-6600 spectrofluorometer. The excitation wavelength was $\lambda_{exc} = 340$ nm.

FTIR spectra were recorded in air at room temperature with a Nicolet 670-FTIR spectrophotometer.

TGA was performed on solid state samples using a Q500 TGA system (TA Instruments) from ambient temperature to 600 °C at a

scan rate of 10 °C/min in air.

Static optical contact angle measurements on the LS coating were performed with an OCA 20 (DataPhysics) equipped with a CCD photo-camera and with a 500-μL Hamilton syringe to dispense liquid droplets. Measurements were taken at room temperature via the sessile drop technique. At least 20 measurements were performed in different regions on the surface of each coating and results were averaged. Water and diiodomethane were used as probe liquids.

PV measurements were performed on DSSC devices having active area of 0.78 cm^2 using a 0.16 cm^2 rigid black mask. I–V electrical characterizations under AM1.5G illumination (100 mW cm^{-2}, or 1 sun) were carried out using a class A solar simulator (91195A, Newport) and a Keithley 2440 source measure unit. All the measurements were carried out on at least three different fresh cells in order to verify the reproducibility of the obtained results, and the experimental results shown in the manuscript are the average of the three replicates. IPCE measurements were performed in DC mode using a 100-W QTH lamp (Newport) as light source and a 150-mm Czerny Turner monochromator (Omni-λ 150, Lot-Oriel, Darmstadt, Germany). As regards devices aging, a standardized protocol for the evaluation of the stability of DSSCs is not present, thus a long-term weathering study was conducted under real outdoor conditions for about 3 months.

3. Results and discussion

In order to obtain the new functional coating system presented in this study, a new UV-curable polymeric precursor was developed, based on a chloro-trifluoro-ethylene vinyl-ether (CTFE-VE) fluoropolymer. In particular, the CTFE-VE polymer was reacted with 2-isocyanatoethyl methacrylate (IEM) to yield a fluoropolymeric precursor bearing photosensitive unsaturated moieties as pendant side groups attached to the main polymer chain. As schematically illustrated in Fig. 2A, this functionalization reaction leads to the formation of urethane bonds from the addition of the $-N=C=O$ groups (IEM) to the $-OH$ groups present in the fluoropolymer, the latter acting in this case as a fluorinated polyol. Upon exposure to UV-light, the methacrylic groups allow the photocrosslinking re-action to occur leading to the formation of the solid polymeric film. Fourier-transform infrared (FTIR) spectroscopy was employed to monitor the extent of the photocrosslinking process by evaluating the variation of absorption intensity of the methacrylate $C=C$ stretching signal in the FTIR spectrum (1636 cm^{-1}) at increasing UV-light exposure time (normalized with respect to the carbonyl $C=O$ stretching signal found at 1720 cm^{-1}). As a result, a conversion curve of the photocrosslinking process was constructed by plotting the ratio between the intensity of the 1636 cm^{-1} FTIR signal at a given UV exposure time and prior to irradiation (Fig. 2B). An over 80% conversion is achieved after 60 s of UV-light exposure, indicating a fast crosslinking process potentially suitable for large scale production. It is worth it to note that this conversion may be underestimated due to the difficulty of a correct quantitative evaluation of the low residual $C=C$ stretching band.

To include a LS functionality to the UV-cured fluoropolymeric coating, a commercial fluorescent organic dye (Lumogen F Violet 570, BASF − from here on referred to as V570) was employed as luminescent doping species because of its high luminescence quantum yield (>95%, [37]), high absorption coefficient (0.1125 mg kg^{-1} cm^{-1} at peak absorption in PMMA), and relatively easy processability with polymers [38]. In order to examine the optical properties of the dye-doped UV-cured LS-coating, UV–vis absorption and fluorescence spectra were collected. As shown in Fig. 3A, a broad absorption band is found in the LS-coating in the
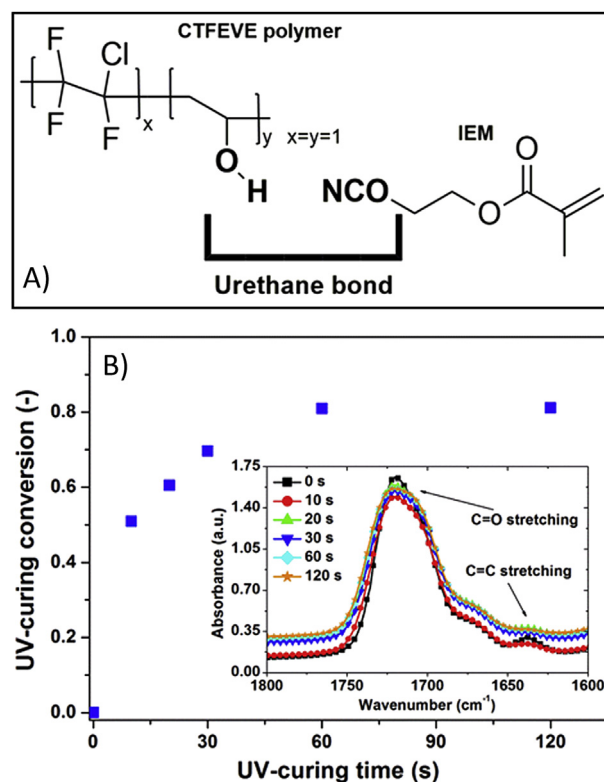

Fig. 2. A) Schematic representation of the reaction between the fluorinated polyol (CTFE-VE) and the functional isocyanate (IEM) used for the preparation of the UV-curable fluorinated precursor; B) Conversion curve for the photocuring process of the LS-coating. The inset shows the FTIR spectra of the photocurable precursor at increasing UV-exposure times in the 1800−1600 cm^{-1} region, indicating the FTIR peaks associated with $C=C$ (1636 cm^{-1}) and $C=O$ (1720 cm^{-1}) stretching vibrations.

325−400 nm range, with an absorption peak centered at 378 nm. The fluorescence spectrum is characterized by a sharp emission centered at 433 nm. These characteristics suggest that the interesting optical features of V570 fluorophore may be exploited to improve the spectral response of DSSC devices in the UV portion of the solar spectrum, where most DSSC dyes perform poorly. In view of this, the indoline-based organic dye D131 (Fig. 3B) was selected as representative Ruthenium-free system to be used in organic DSSC devices in combination with the new V570-doped LS-coating presented in this work. As evident from Fig. 3A, the presence of V570 in the LS-coating allows for improved light harvesting in the 325−400 nm spectral range where D131 shows an absorption minimum, and promotes a 55-nm red-shifted emission in the spectral region where D131 shows an absorption maximum.

To evaluate the effect of this excellent spectral matching on PV performance, DSSC devices were fabricated by sandwiching a D131-sensitized TiO_2 mesoporous anode, an iodide/triiodide liquid electrolyte and a Pt-sputtered counter electrode. The LS film was spin-coated on the external side of PV cell photoanode (Fig. 1A), and the effect of increasing amounts of V570 incorporated in the photopolymer on the performance of the DSSC devices was thoroughly investigated.

The PV response of the LS-DSSC system at increasing V570 concentration is reported in Fig. 4, where the clearly positive effect of the LS-coating on DSSC performance can be noticed on all characteristic PV parameters. To begin with, a strong improvement of short circuit photocurrent density (J_{sc}, Fig. 4A) was achieved. In detail, a 15% J_{sc} enhancement was observed in the presence of 0.75 wt% V570 with respect to uncoated devices, rising up to 135%
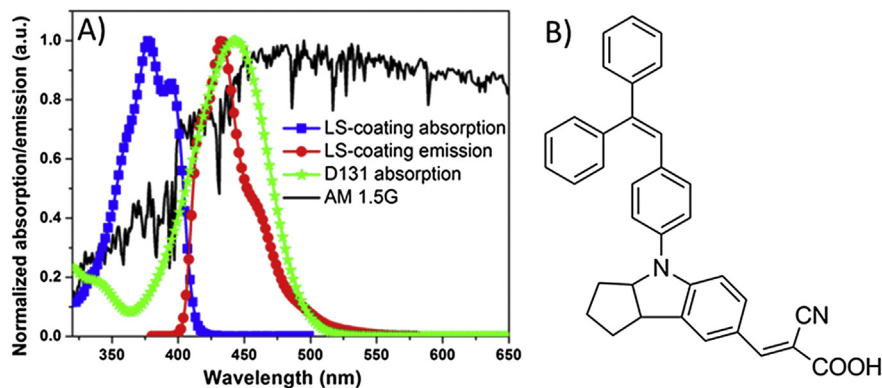
Fig. 3. A) Normalized absorption and emission spectra of the LS-coating presented in this work. The absorption of the organic dye D131 and the AM1.5G solar emission spectrum are also shown; B) Chemical structure of the organic sensitizer D131 used in this work for the fabrication of DSSC devices.
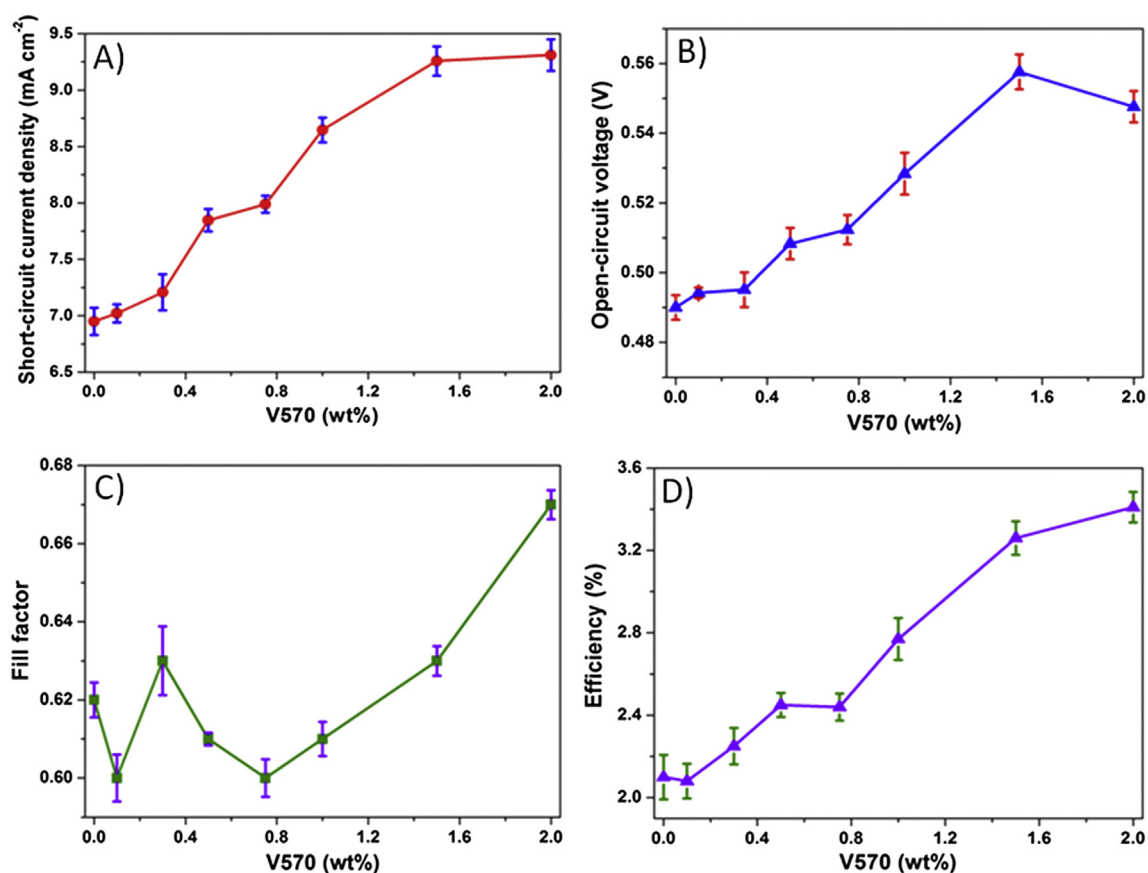

Fig. 4. Variation of PV parameters of LS-DSSC devices at increasing concentration of V570 luminescent species: A) Short circuit current density (J_{sc}); B) Open circuit voltage (V_{oc}); C) Fill factor (FF); D) Efficiency (η).

in the presence of 2 wt% V570 luminophore in the crosslinked polymeric film. These data confirmed that the adopted luminescent material is effectively able to convert at the nanoscale the region of the solar spectrum peaked at 378 nm into lower-energy photons of wavelengths well matching the absorption spectrum of D131 (Fig. 3A). The latter phenomenon is easily noticeable by observing the incident photon-to-current efficiency (IPCE) curves reported in Fig. 5A. Here, the increased amount of photons harvested by the D131 dye due to the presence of the LS-coating led to increased IPCE values in the spectral region where the absorption of the luminophore V570 is centered (378 nm). The optical effect resulting

from the incorporation of a LS agent in the new polymeric matrix presented in this work can also be clearly appreciated in Fig. 1B. The integration of the product of the AM1.5G photon flux with the IPCE spectrum yielded predicted J_{sc} values equal to 6.87, 8.04 and 9.25 mA cm^{-2} for the LS-free and LS-coated (0.75 and 2.0 wt%) DSSCs, respectively, which are in excellent agreement with the measured values reported in the photocurrent-photovoltage (J−V) curves in Fig. 5B.

Data reported in Fig. 4A show that a plateau J_{sc} value is reached for V570 concentrations in the 1.5−2 wt% range. With the aim of further investigating the effect of fluorophore concentration and
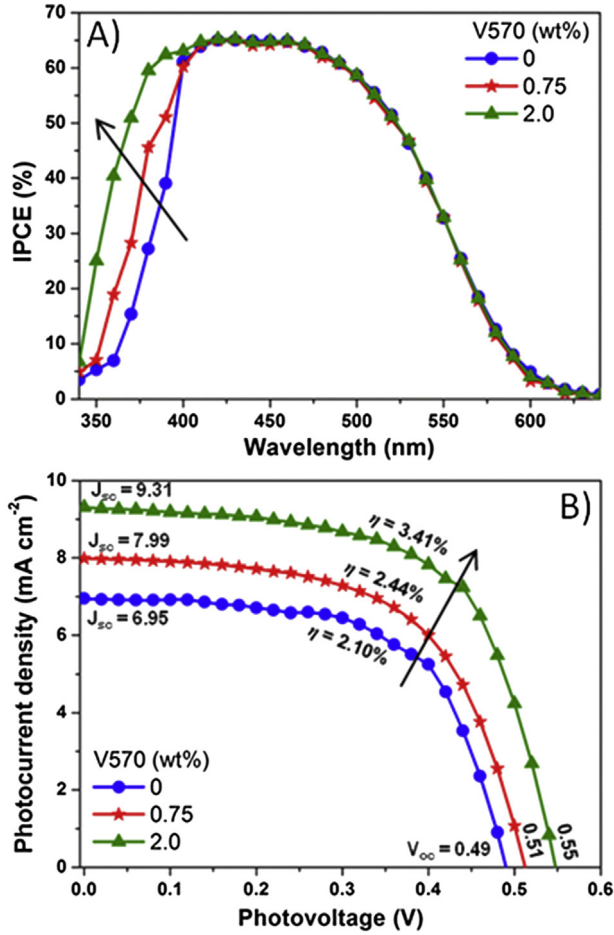
Fig. 5. A) IPCE curves of LS-DSSCs at increasing concentration of V570 luminescent species; B) J–V curves of LS-DSSCs at increasing concentration of V570 luminescent species. Reported J_{sc} and V_{oc} values are expressed in mA cm^{-2} and V, respectively.

thus extending the experimental domain we also produced DSSC devices incorporating a 5 wt% V570-doped LS coating. However, a decrease of J_{sc} from 9.31 mA cm^{-2} (2 wt% V570) to 8.48 mA cm^{-2} (5 wt% V570) was observed. This behavior may be explained by considering two concurrent effects taking place at increasing fluorophore concentrations. A higher concentration of fluorescent species may increase the probability for an emitted photon to be re-absorbed by another adjacent fluorophore molecule in the LS film, due to the partial overlap between absorption and emission spectra of V570 dye (Fig. 3A) and because of the decreasing fluorophore-to-fluorophore intermolecular distance with increasing V570 con-centration. Additionally, an increased concentration of fluorescent species in the LS coating may result in the formation of molecular aggregates (dimers and excimers), that were shown on similar systems to promote fluorescence quenching [39,40]. These two parallel phenomena may be responsible for a lower amount of fluorescence photons emitted by the LS coating to reach the un-derlying DSSC photoactive layer for PV conversion, thus leading to a performance (J_{sc}) decrease at higher V570 concentrations. Finally, the progressively higher optical density of the LS coating at increasing V570 concentration may also cause a reduction of the amount of long-wavelength photons reaching the DSSC device due to decreased coating transmittance, ultimately leading to an overall decrease in PV performance. This effect is clearly visible at fluo-rophore concentrations higher than 2 wt% (see Fig. A.1 in the Ap-pendix A).

While the increase of photocurrent density could be reasonably expected in the presence of a LS coating, it was quite surprising to note that also the open-circuit voltage (V_{oc}) was slightly improved with increasing V570 concentration (see Fig. 4B). There is a general agreement within the DSSC scientific community about the dependence of V_{oc} on the electrolyte composition and on the modification of electrodes/electrolyte interfaces [41,42]. However, the same components were used for the fabrication of all the DSSC devices presented in this work, while the only variable was the concentration of the luminescent agent. We speculate that the trend observed on V_{oc} may be due to a thermal effect induced by the presence of the LS coating. Indeed, a decrease of V_{oc} is usually caused by the increase of the dark current attributed to the triio-dide reduction by conduction band electrons at the semi-conductor−electrolyte junction [43]. Such a process is enhanced when temperature rises. Indeed, in this system the recombination resistance (R_{rec}) follows the relation

$$R_{rec} = R_0 \cdot exp\left(-\frac{\beta \cdot q}{k_B \cdot T} \cdot V_F \right) \qquad (1)$$

where β is a coefficient associated with the non-linearity of the charge transfer process and equivalent to the non-ideality factor ($m = \beta^{-1}$) of the diode equation used for standard semiconductor solar cells, q is the electron charge, k_B the Boltzmann constant, T the absolute temperature, V_f the potential drop in the TiO$_2$ film, and R_0 the pre-exponential parameter which results from the relation

$$R_0 = \frac{T_0 \cdot \sqrt{\pi \cdot \lambda \cdot k_B \cdot T}}{q^2 \cdot L \cdot k_0 \cdot c_{ox} \cdot N_s \cdot T} \cdot exp\left(\frac{E_c - E_{redox}}{k_B \cdot T_0} + \frac{\lambda}{4 k_B \cdot T} \right) \qquad (2)$$

where λ is the reorganization energy, L the film thickness, k_0 a time constant for tunneling (rate constant), c_{ox} the concentration of acceptor species in the electrolyte, N_s the density of states near the TiO$_2$ surface, E_c the conduction band position of TiO$_2$, and T_0 a parameter with temperature units determining the depth of the trap distribution tail under the conduction band [44,45]. This model agrees well with a recombination process occurring through extended surface states in an energy tail distributed below the conduction band, which follows the Marcus probabilistic model [46]. As a consequence, the decrease usually observed in R_{rec} with increasing temperature is associated with a decrease in R_0 and is responsible for the onset of current loss that occurs at lower po-tentials [47]. Therefore, the increased V_{oc} values observed for the coated DSSCs may be the result of two different phenomena. First, the fluoropolymeric coating deposited on the light-exposed face of the DSSC device is able to absorb hot IR photons of the solar spectrum, thus reducing device operating temperature. Indeed, fluoropolymers are characterized by a strong and wide absorption band in the IR region of the electromagnetic spectrum, which re-sults from the C−F bond stretching vibration [48]. This character-istic behavior may lead to increased R_0 and R_{rec} and in turn to enhanced V_{oc}. As a second effect, the presence of increasing amount of fluorophore in the LS coating partially shields the DSSC device from harmful near UV photons, which are known to cause photo-oxidation of some DSSC components and lead to the formation of radical species or organic by-products that could act as electron acceptors at the electrolyte/photoanode interface [49]. The UV-shielding effect imparted by the LS coating may limit the forma-tion of such electron acceptor species in the electrolyte (c_{ox}), thus resulting in increased R_0, R_{rec} and V_{oc}. Moreover, such a reduction of the recombination phenomena also resulted in a slight improve-ment of fill factor (*FF*) values (Fig. 4C), as already reported by pre-vious studies about thermal effects on the PV performance [50].

The effect of the LS coating on the PV parameters as described

above led to a maximum overall sunlight to electricity conversion efficiency (η) improvement of 62% with respect to uncoated DSSC devices. As reported in Fig. 4D, device performance increased from 2.10% to 3.41% when a 2 wt% V570-laden LS coating was used. To the best of our knowledge, this value represents the highest efficiency enhancement reported so far for organic DSSC systems by means of a polymeric LS layer doped with an organic fluorophore. This very positive result appears even more remarkable when considering that the LS coating has been applied through a cheap, straightfor-ward and easily up-scalable process of light-induced polymeriza-tion, carried out at room temperature and without the use of catalysts or separation/purification steps. Moreover, a slight anti-reflective behavior was conferred to the photoanode (see Fig. A.2 in the Appendix A).

For particular purposes, such as flexible PV cells [51], aerospace applications [52] and power stations [53], device transparency is not required. Thus, the use of back-reflective surfaces (BRSs) on the rear of the PV cells may represent an interesting option to increase the photon flux available for the PV device. In fact, if the DSSC components (coating, conductive glass, photoanode, electrolyte and cathode) are sufficiently transparent, the photons unabsorbed by the sensitizer are reflected by the BRS and sent back to the sensitizer. In this work, we also assembled the 2 wt% V570-laden LS-DSSC ($\eta = 3.41\%$) with a BRS positioned on the counter elec-trode side. An efficiency as high as 5.02% ($J_{sc} = 13.62$ mA cm^{-2}, $V_{oc} = 0.55$ V, $FF = 0.67$) was obtained, thereby confirming the excellent transparency of the LS coating (and also of the other components used for fabricating the DSSC devices) and its suit-ability to be used in applications in which a BRS is involved [54].

In addition to providing excellent transparency and relatively good solubility of the fluorescent species, the choice of the new fluoropolymeric coating proposed in this work was also driven by the need of ensuring long-term durability of the operating device. In fact, a decrease in device efficiency is usually observed during the first weeks of DSSC device lifetime, and this issue represents a serious drawback for the widespread application of this technology [55]. In recent years, this aspect has forced the scientific community to propose new materials to reduce the volatility of the liquid electrolyte [56,57] and to protect cell components from the action of UV light, heat and meteorological phenomena [58]. In this context, the use of fluoropolymeric coatings for outdoor applica-tions may represent an interesting approach to ensure high weathering resistance and long-term durability of DSSC devices, due to the excellent weatherability characteristics given to fluori-nated polymers by the higher strength of the carbon−fluorine bond compared to the carbon−hydrogen bond [20,21].

With the aim of verifying under real operative conditions the performance of the fluoropolymeric coating presented in this work, an intensive device aging study was carried out. A long-term weathering study on control bare DSSCs and LS-DSSCs was con-ducted in real outdoor conditions for three months (2140 h), during which the PV cells were exposed (day and night) in the garden of the DISAT building in Turin (45°03′42.0″N, 7°39′48.1″E), located in northern Italy in a humid subtropical climate zone. Thanks to this choice, all the DSSC devices were subjected to highly variable cli-matic conditions, which are particularly useful for our purpose, i.e. to carry out a realistic long-term study of DSSC aging. During the first quarter of 2014 (February−April), outdoor temperatures ranged from −2 to 32 °C and about 350 mm of accumulated rain were measured by the local environmental protection agency (Arpa Piemonte) [59]. The comparison between the aging test on coated (2 wt% V570) and control devices is reported in Fig. 6A. Together with the data plotted in Fig. 4, it is clear how the proposed lumi-nescent coating not only produced a great improvement of DSSCs performance, but also imparted an excellent long-term stability to

the DSSC device under real outdoor conditions, the latter repre-senting an aspect of paramount importance for the practical exploitation of this kind of third generation PV technology. In detail, while the control device (V570 0 wt%) lost about 30% of its initial efficiency, the LS-DSSC system (V570 2.0 wt%) preserved 93% of its starting performance.

The strong improvement of long-term stability under real out-door conditions observed when the LS coating was applied to the DSSC device may be ascribed to the action of three combined fac-tors. Firstly, the coating showed easy-cleaning properties due to its fluorinated nature. Static contact angle measurements performed on the LS coating to investigate its wettability behavior revealed the fairly hydrophobic character of the new fluoropolymeric coating. As can be appreciated in Fig. 6B, a remarkable increase of water con-tact angle θ_{H2O} and a decrease of surface tension γ were observed when the outer DSSC glass was coated with the new fluoropoly-meric LS system. Such behavior allows to keep the external side of the photoanode clean, thus avoiding the decrease of device photocurrent likely caused by the formation of physical barriers (dust, dirt, water residues) that may prevent incident solar photons from reaching the D131-sensitized electrode for PV conversion. Secondly, the hydrophobic nature of the coating applied on the device may contribute to hinder a very important and widespread degradation phenomenon observed in DSSC systems, i.e. the permeation of water into the device that is often found to alter the composition and the correct functionality of photoanode and electrolyte [60]. Finally, we previously showed that the lumines-cent species present in the LS coating can act as a light-shifter, thus also serving the function of a UV filter. As a consequence, the remarkable aging resistance shown by the LS-DSSC systems is also attributable to the reduction of the light-induced degradation phenomena normally occurring during outdoor exposure to the photosensitive components of DSSC devices, especially to dye, redox couple and electrolyte additives [61]. The excellent thermal stability of the fluoropolymeric system used as carrier matrix (see Fig. A.3 Appendix A for the thermogravimetric analysis of the coating) combined with its intrinsic photooxidative stability further contribute to enhance the lifetime of LS-DSSC systems.

All the present findings clearly highlight the multifunctional nature of the here-proposed LS coating, whose excellent barrier properties to the meteorological phenomena (occurred during the aging test) are also evident from a visual inspection of control and LS-DSSC devices after long-term outdoor exposure (see Fig. A.4 in the Appendix A).

4. Conclusions

In conclusion, for the first time a fluoropolymeric and rare elements-free LS coating system was designed, synthesized and characterized for use in organic DSSC devices. By the introduction of a fluorescent species in a newly proposed fluoropolymeric ma-trix, down-shifting of UV photons into valuable visible light has been achieved. As a consequence, DSSCs incorporating the coating system showed an over 60% relative increase in photovoltaic effi-ciency, mainly caused by the increased photon flux harvested by the organic dye resulting from the nanometric light shifting effect promoted by the luminescent agent. Furthermore, a long-term weathering study was performed under real outdoor conditions, and DSSCs incorporating the LS coating were found to nearly fully preserve their initial power conversion efficiency, as opposed to control devices that showed a 26% relative efficiency loss. Such a remarkable outdoor stability observed for LS-DSSCs was attributed to the multipurpose behavior of the LS layer. Indeed, such new coating system was able to act both as a UV-screening agent (thus preserving the photosensitive PV cell components) and as an easy-
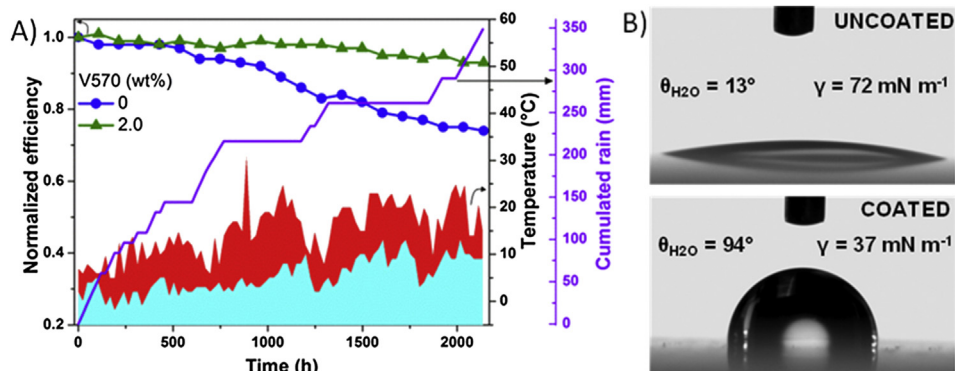
Fig. 6. A) Stability test carried out on LS-free and LS-coated (2 wt% V570) DSSCs in real outdoor conditions. The lower part of the graph shows the outdoor temperatures (minimum and maximum) registered during the testing period, while the violet curve shows the accumulated rainfall; B) Static contact angles (θ_{H2O}) and total surface tension values (γ) for bare glass and glass coated with the LS film. (For interpretation of the references to colour in this figure legend, the reader is referred to the web version of this article.)

cleaning layer (by keeping the PV cell clean and preventing water permeation). This study clearly demonstrates that it is possible to simultaneously improve performance and weatherability of organic DSSC devices, and may be readily extended to a large variety of sensitizer/luminophore combinations as well as to the nascent world of perovskite solar cells, whose instability to humidity and near-UV radiation represents one of the major problems currently under intense investigation [62].

Appendix A. Supplementary data

Supplementary data related to this article can be found on line.

References

[1] M. Grätzel, Dye-sensitized solar cells, J. Photochem. Photobiol. C 4 (2003) 145–153.

[2] B.C. O'Regan, M. Grätzel, A low-cost, high-efficiency solar cell based on dye-sensitized colloidal TiO_2 films, Nature 353 (1991) 737–740.

[3] F. Bella, A. Sacco, D. Pugliese, M. Laurenti, S. Bianco, Additives and salts for dye-sensitized solar cells electrolytes: what is the best choice? J. Power Sources 364 (2014) 333–343.

[4] S. Mathew, A. Yella, P. Gao, R. Humphry-Baker, B.F.E. Curchod, N. Ashari-Astani, I. Tavernelli, U. Rothlisberger, M.K. Nazeeruddin, M. Grätzel, Dye-sensitized solar cells with 13% efficiency achieved through the molecular engineering of porphyrin sensitizers, Nat. Chem. 6 (2014) 242–247.

[5] Y. Duan, Q. Tang, R. Li, B. He, L. Yu, An avenue of sealing liquid electrolyte in flexible dye-sensitized solar cells, J. Power Sources 274 (2015) 304–309.

[6] Z. Wang, Q. Tang, B. He, X. Chen, H. Chen, L. Yu, Titanium dioxide/calcium fluoride nanocrystallite for efficient dye-sensitized solar cell. A strategy of enhancing light harvest, J. Power Sources 275 (2015) 175–180.

[7] W. Guo, X. Xue, S. Wang, C. Lin, Z.L. Wang, An integrated power pack of dye-sensitized solar cell and Li battery based on double-sided TiO_2 nanotube arrays, Nano Lett. 12 (2012) 2520–2523.

[8] S. Ahmad, E. Guillén, L. Kavan, M. Grätzel, M.K. Nazeeruddin, Metal free sensitizer and catalyst for dye sensitized solar cells, Energy Environ. Sci. 6 (2013) 3439–3466.

[9] K. Kakiage, Y. Aoyama, T. Yano, T. Otsuka, T. Kyomen, M. Unno, M. Hanaya, An achievement of over 12 percent efficiency in an organic dye-sensitized solar cell, Chem. Commun. 50 (2014) 6379–6381.

[10] K. Ali, S.A. Khan, M.Z. Mat Jafri, Enhancement of silicon solar cell efficiency by using back surface field in comparison of different antireflective coatings, Sol. Energy 101 (2014) 1–7.

[11] P.M. Kaminski, F. Lisco, J.M. Walls, Multilayer broadband antireflective coatings for more efficient thin film CdTe solar cells, IEEE J. Photovolt. 4 (2014) 452–456.

[12] L. Yao, J. He, Recent progress in antireflection and self-cleaning technology - from surface engineering to functional surfaces, Prog. Mater. Sci. 61 (2014) 94–143.

[13] P. Šiffalovič, M. Jergel, M. Benkovičová, A. Vojtko, V. Nádaždy, J. Ivančo, M. Bodík, M. Demydenko, E. Majková, Towards new multifunctional coatings for organic photovoltaics, Sol. Energy Mater. Sol. Cells 125 (2014) 127–132.

[14] L. Miao, L.F. Su, S. Tanemura, C.A.J. Fisher, L.L. Zhao, Q. Liang, G. Xu, Cost-effective nanoporous SiO_2-TiO_2 coatings on glass substrates with antireflective and self-cleaning properties, Appl. Energy 112 (2013) 1198–1205.

[15] N. Jiang, T. Sumitomo, T. Lee, A. Pellaroque, O. Bellon, D. Milliken, H. Desilvestro, High temperature stability of dye solar cells, Sol. Energy Mater. Sol. Cells 119 (2013) 36–50.

[16] J.T. Park, J.H. Kim, D. Lee, Excellent anti-fogging dye-sensitized solar cells based on superhydrophilic nanoparticle coatings, Nanoscale 6 (2014) 7362–7368.

[17] S.Y. Heo, J.K. Koh, G. Kang, S.H. Ahn, W.S. Chi, K. Kim, J.H. Kim, Bifunctional moth-eye nanopatterned dye-sensitized solar cells: light-harvesting and self-cleaning effects, Adv. Energy Mater. 4 (2014) 1300632.

[18] J. Scheirs, Modern Fluoropolymers: High Performance Polymers for Diverse Applications, John Wiley & Sons Ltd, Chichester, 1997.

[19] D.M. Lemal, Perspective on fluorocarbon chemistry, J. Org. Chem. 69 (2004) 1–11.

[20] D. O'Hagan, Understanding organofluorine chemistry. An introduction to the C–F bond, Chem. Soc. Rev. 37 (2008) 308–319.

[21] G. Couture, B. Campagne, A. Alaaeddine, B. Ameduri, Synthesis and characterizations of alternating co- and terpolymers based on vinyl ethers and chlorotrifluoroethylene, Polym. Chem. 4 (2013) 1960–1968.

[22] G. Griffini, M. Levi, S. Turri, Novel high-durability luminescent solar concentrators based on fluoropolymer coatings, Progr. Org. Coat. 77 (2014) 528–536.

[23] G. Griffini, M. Levi, S. Turri, Novel crosslinked host matrices based on fluorinated polymers for long-term durability in thin-film luminescent solar concentrators, Sol. Energy Mater. Sol. Cells 118 (2013) 36–42.

[24] G. Griffini, L. Brambilla, M. Levi, C. Castiglioni, M. Del Zoppo, S. Turri, Anthracene/tetracene cocrystals as novel fluorophores in thin-film luminescent solar concentrators, RSC Adv. 4 (2014) 9893–9897.

[25] F. Bella, R. Bongiovanni, R.S. Kumar, M.A. Kulandainathan, A.M. Stephan, Light cured networks containing metal organic frameworks as efficient and durable polymer electrolytes for dye-sensitized solar cells, J. Mater. Chem. A 1 (2013) 9033–9036.

[26] J.D. Douglas, G. Griffini, T.W. Holcombe, E.P. Young, O.P. Lee, M.S. Chen, J.M.J. Fréchet, Functionalized isothianaphthene monomers that promote quinoidal character in donor-acceptor copolymers for organic photovoltaics, Macromolecules 45 (2012) 4069–4074.

[27] G. Griffini, J.D. Douglas, C. Piliego, T.W. Holcombe, S. Turri, J.M.J. Fréchet, J.L. Mynar, Long-term thermal stability of high-efficiency polymer solar cells based on photocrosslinkable donor-acceptor conjugated polymers, Adv. Mater. 23 (2011) 1660–1664.

[28] M.N. Huang, Y.Y. Ma, F. Xiao, Q.Y. Zhang, Bi^{3+} sensitized Y_2WO_6:Ln^{3+} (Ln = Dy, Eu, and Sm) phosphors for solar spectral conversion, Spectrochim. Acta Part A 120 (2014) 55–59.

[29] Z. Hosseini, W.K. Huang, C.M. Tsai, T.M. Chen, N. Taghavinia, E.W. Diau, Enhanced light harvesting with a reflective luminescent down-shifting layer for dye-sensitized solar cells, ACS Appl. Mater. Interf. 5 (2013) 5397–5402.

[30] Y. Li, K. Pan, G. Wang, B. Jiang, C. Tian, W. Zhou, Y. Qu, S. Liu, L. Feng, H. Fu, Enhanced photoelectric conversion efficiency of dye-sensitized solar cells by the incorporation of dual-mode luminescent $NaYF_4$:Yb^{3+}/Er^{3+}, Dalton Trans. 42 (2013) 7971–7979.

[31] J. Wang, J. Wu, J. Lin, M. Huang, Y. Huang, Z. Lan, Y. Xiao, G. Yue, S. Yin, T. Sato, Application of Y_2O_3:Er^{3+} nanorods in dye-sensitized solar cells, Chem-SusChem 5 (2012) 1307–1312.

[32] J. Liu, Q. Yao, Y. Li, Effects of downconversion luminescent film in dye-sensitized solar cells, Appl. Phys. Lett. 88 (2006) 173119.

[33] G. Griffini, F. Bella, F. Nisic, C. Dragonetti, D. Roberto, M. Levi, R. Bongiovanni, S. Turri, Multifunctional luminescent down-shifting fluoropolymer coatings: a straightforward strategy to improve the UV-light harvesting ability and long-term outdoor stability of organic dye-sensitized solar cells, Adv. Energy Mater. 5 (2015), http://dx.doi.org/10.1002/aenm.201401312 article number (1401312).

[34] L.Y. Lin, M.H. Yeh, C.P. Lee, J. Chang, A. Baheti, R. Vittal, K.R. Justin Thomas, K.C. Ho, Insights into the co-sensitizer adsorption kinetics for complementary

organic dye-sensitized solar cells, J. Power Sources 247 (2014) 906–914.

[35] S. Kumar Swami, N. Chaturvedi, A. Kumar, R. Kapoor, V. Dutta, J. Frey, T. Moehl, M. Grätzel, S. Mathew, M.K. Nazeeruddin, Investigation of electro-deposited cobalt sulphide counter electrodes and their application in next-generation dye sensitized solar cells featuring organic dyes and cobalt-based redox electrolytes, J. Power Sources 275 (2015) 80–89.

[36] S.K. Pathak, A. Abate, T. Leijtens, D.J. Hollman, J. Teuscher, L. Pazos, P. Docampo, U. Steiner, H.J. Snaith, Towards long-term photostability of solid-state dye sensitized solar cells, Adv. Energy Mater. 4 (2014) 1301667.

[37] D. Ross, E. Klampaftis, J. Fritsche, M. Bauer, B.S. Richards, Increased short-circuit current density of production line CdTe mini-module through luminescent down-shifting, Sol. Energy Mater. Sol. Cells 103 (2012) 11–16.

[38] L.R. Wilson, B.S. Richards, Measurement method for photoluminescent quantum yields of fluorescent organic dyes in polymethyl methacrylate for luminescent solar concentrators, Appl. Opt. 48 (2009) 212–220.

[39] R.O. Al Kaysi, T.S. Ahn, A.M. Muller, C.J. Bardeen, The photophysical properties of chromophores at high (100 mM and above) concentrations in polymers and as neat solids, Phys. Chem. Chem. Phys. 8 (2006) 3453–3459.

[40] H. Yoo, J. Yang, A. Yousef, M.R. Wasielewski, D. Kim, Excimer formation dynamics of intramolecular pi-stacked perylenediimides probed by single-molecule fluorescence spectroscopy, J. Am. Chem. Soc. 132 (2010) 3939–3944.

[41] T. Chen, L. Qiu, Z. Cai, F. Gong, Z. Yang, Z. Wang, H. Peng, Intertwined aligned carbon nanotube fiber based dye-sensitized solar cells, Nano Lett. 12 (2012) 2568–2572.

[42] S.J. Park, K. Yoo, J.Y. Kim, J.Y. Kim, D.K. Lee, B.S. Kim, H. Kim, J.H. Kim, J. Cho, M.J. Ko, Water-based thixotropic polymer gel electrolyte for dye-sensitized solar cells, ACS Nano 7 (2013) 4050–4056.

[43] G. Boschloo, A. Hagfeldt, Characteristics of the iodide/triiodide redox mediator in dye-sensitized solar cells, Acc. Chem. Res. 42 (2009) 1819–1826.

[44] Q. Wang, S. Ito, M. Grätzel, F. Fabregat-Santiago, I. Mora-Seró, J. Bisquert, T. Bessho, H. Imai, Characteristics of high efficiency dye-sensitized solar cells, J. Phys. Chem. B 110 (2006) 19406–19411.

[45] S.R. Raga, F. Fabregat-Santiago, Temperature effects in dye-sensitized solar cells, Phys. Chem. Chem. Phys. 15 (2013) 2328–2336.

[46] R. Memming, Semiconductor Electrochemistry, Wiley-VCH, Weinheim, 2001.

[47] F. Fabregat-Santiago, G. Garcia-Belmonte, I. Mora-Seró, J. Bisquert, Characterization of nanostructured hybrid and organic solar cells by impedance spectroscopy, Phys. Chem. Chem. Phys. 13 (2011) 9083–9118.

[48] G. Hougham, P.E. Cassidy, K. Johns, T. Davidson, Fluoropolymers 2. Properties, Kluwer Academic/Plenum Publishers, Dordrecht, 1999.

[49] S. Mastroianni, I. Asghar, K. Miettunen, J. Halme, A. Lanuti, T.M. Brown, P. Lund, Effect of electrolyte bleaching on the stability and performance of dye solar cells, Phys. Chem. Chem. Phys. 16 (2014) 6092–6100.

[50] P.J. Li, J.H. Wu, M.L. Huang, S.C. Hao, Z. Lan, Q. Li, S. Kang, The application of P(MMA-co-MAA)/PEG polyblend gel electrolyte in quasi-solid state dye-sensitized solar cell at higher temperature, Electrochim. Acta 53 (2007) 903–908.

[51] F. Bella, A. Lamberti, A. Sacco, S. Bianco, A. Chiodoni, R. Bongiovanni, Novel electrode and electrolyte membranes: towards flexible dye-sensitized solar cell combining vertically aligned TiO_2 nanotube array and light-cured polymer network, J. Membr. Sci. 470 (2014) 125–131.

[52] J.D. Harris, E.J. Anglin, A.F. Hepp, S.G. Bailey, D.A. Scheiman, S.L. Castro, Space Environmental Testing of Dye-sensitized Solar Cells, Eur. Space Agency Spec. Publ. SP 502, 2002, pp. 629–632.

[53] S. Dai, J. Weng, Y. Sui, S. Chen, S. Xiao, Y. Huang, F. Kong, X. Pan, L. Hu, C. Zhang, K. Wang, The design and outdoor application of dye-sensitized solar cells, Inorg. Chim. Acta 361 (2008) 786–791.

[54] V. Zardetto, F. Di Giacomo, D. Garcia-Alonso, W. Keuning, M. Creatore, C. Mazzuca, A. Reale, A. Di Carlo, T.M. Brown, Fully plastic dye solar cell devices by low-temperature UV-irradiation of both the mesoporous TiO_2 photo- and platinized counter-electrodes, Adv. Energy Mater. 3 (2013) 1292–1298.

[55] L. Tao, Z. Huo, S. Dai, J. Zhu, C. Zhang, Y. Huang, B. Zhang, J. Yao, Stable quasi-solid-state dye-sensitized solar cell using a diamide derivative as low molecular mass organogelator, J. Power Sources 262 (2014) 444–450.

[56] X. Wang, S.A. Kulkarni, B.I. Ito, S.K. Batabyal, K. Nonomura, C.C. Wong, M. Grätzel, S.G. Mhaisalkar, S. Uchida, Nanoclay gelation approach toward improved dye-sensitized solar cell efficiencies: an investigation of charge transport and shift in the TiO_2 conduction band, ACS Appl. Mater. Interf. 5 (2013) 444–450.

[57] A. Hess, G. Barber, C. Chen, T.E. Mallouk, H.R. Allcock, Organophosphates as solvents for electrolytes in electrochemical devices, ACS Appl. Mater. Interf. 5 (2013) 13029–13034.

[58] K. Darowicki, M. Szociński, K. Schaefer, D.J. Mills, The influence of UV light on performance of poly(methyl methacrylate) in regard to dye-sensitised solar cells, ECS Trans. 24 (2010) 127–136.

[59] Arpa Piemonte [Regional agency for environmental protection] website, http://www.arpa.piemonte.it/rischinaturali/tematismi/clima/rapporti-di-analisi/Eventi.html. [accessed: June, 2014].

[60] Y. Liu, A. Hagfeldt, X.R. Xiao, S.E. Lindquist, Investigation of influence of redox species on the interfacial energetics of a dye-sensitized nanoporous TiO_2 solar cell, Sol. Energy Mater. Sol. Cells 55 (1998) 267–281.

[61] J.S. Lissau, D. Nauroozi, M.P. Santoni, S. Ott, J.M. Gardner, A. Morandeira, Anchoring energy acceptors to nanostructured ZrO_2 enhances photon upconversion by sensitized triplet-triplet annihilation under simulated solar flux, J. Phys. Chem. C 117 (2013) 14493–14501.

[62] M.A. Green, A. Ho-Baillie, H.J. Snaith, The emergence of perovskite solar cells, Nat. Photonics 8 (2014) 506–514.